NANO LETTERS

2008
Vol. 8, No. 11
4027-4032

Integrated Multilayer Nanogenerator Fabricated Using Paired Nanotip-to-Nanowire Brushes

Sheng Xu,† Yaguang Wei,† Jin Liu, Rusen Yang, and Zhong Lin Wang*

School of Materials Science and Engineering, Georgia Institute of Technology, Atlanta, Georgia 30332-0245

Received September 12, 2008; Revised Manuscript Received October 4, 2008

ABSTRACT

We present a new approach to a nanogenerator (NG) that is composed of integrated, paired nanobrushes made of pyramid-shaped metal-coated ZnO nanotip (NTP) arrays and hexagonal-prism-shaped ZnO nanowire (NW) arrays, which were synthesized using a chemical approach at <100 °C on the two surfaces of a common substrate, respectively. The operation of the NGs relies on mechanical deflection/bending of the NWs, in which resonance of NWs is not required to activate the NG. This largely expands the application of the NGs from low frequency (approximately the hertz range) to a relatively high frequency (approximately the megahertz range) for effectively harvesting mechanical energies in our living environment. With one piece of such a structure stacked in close proximity over another to form a layer-by-layer matched brush architecture, direct current is generated by exciting the architecture using ultrasonic waves. A four-layer integrated NG is demonstrated to generate an output power density of 0.11 μW/cm^2 at 62 mV. The layer-by-layer assembly provides a feasible technology for building three-dimensional NGs for applications where force or pressure variations are available, such as a shoe pad, an underskin layer for airplanes, and next to a vibration source such as a car engine or tire.

Building self-powered nanosystems is a future direction of nanotechnology. A nanosystem is an integration of nanodevices, functional components, and a power source. Energy harvesting from the environment for powering a nanosystem is vitally important for its independent, wireless, and sustainable operation.[1,2] A piezoelectric nanogenerator (NG) is a promising approach for this application. The NG is based on a vertically aligned ZnO nanowire (NW) array that is placed beneath a zigzag electrode with a small gap.[3] The NG relies on the piezoelectric potential created in a NW once subject to elastic straining, which drives the flow of charge carriers.[4] The zigzag electrode acts as an array of parallel integrated tips for simultaneously creating, collecting, and outputting electricity from all of the active NWs. In this design, the nonuniform heights and random distribution of the NWs on a substrate, however, may prevent a large fraction of NWs from contributing to the energy conversion process; the packaging technology is of critical importance to keep the gap distance between the zigzag electrode and the NW arrays just right so that it is large enough to allow the NWs to be freely bent/deflected but small enough to ensure an intimate contact between the NWs and the electrode.[5,6]

In this paper, we present a new approach to a NG that is composed of integrated, paired nanobrushes made of pyramid-shaped metal-coated ZnO nanotip (NTP) arrays and hexagonal-prism-shaped ZnO NW arrays, which were synthesized using a chemical approach at <100 °C on the two surfaces of a common substrate, respectively. When one piece of such structure is stacked in close proximity over another to form a layer-by-layer matched brush architecture, direct current is generated by exciting the architecture using ultrasonic waves. A four-layer integrated NG is demonstrated to generate an output power density of 0.11 μW/cm^2 at a voltage of 62 mV.

The NGs were first fabricated by rationally growing ZnO arrays of controlled orientation and shape on a double-side polished Si wafer (Figure S1a).[7,8] The wafer was coated with 100 nm thick Al_2O_3 film on both sides by atomic layer deposition (Figure S1b), which served as an insulating layer to ensure independent operations of the NGs to be built in the adjacent layers. Then the wafer was deposited with a 20 nm thick Cr layer by direct current magnetron plasma sputtering on both the top and bottom surfaces except the side surface (Figure S1c). Following that, a 50 nm thick ZnO layer was deposited by radio frequency magnetron sputtering onto the Cr layers at the top and bottom surfaces except side surfaces (Figure S1d). The Cr layer served not only as an adhesion to bind the Al_2O_3 layer and the ZnO layer together but also as a common electrode for collecting the charges to be transported through each and every active NW/NTP.

* Corresponding author, zlwang@gatech.edu.
† These authors contributed equally to this work.

10.1021/nl8027813 CCC: $40.75
Published on Web 10/22/2008

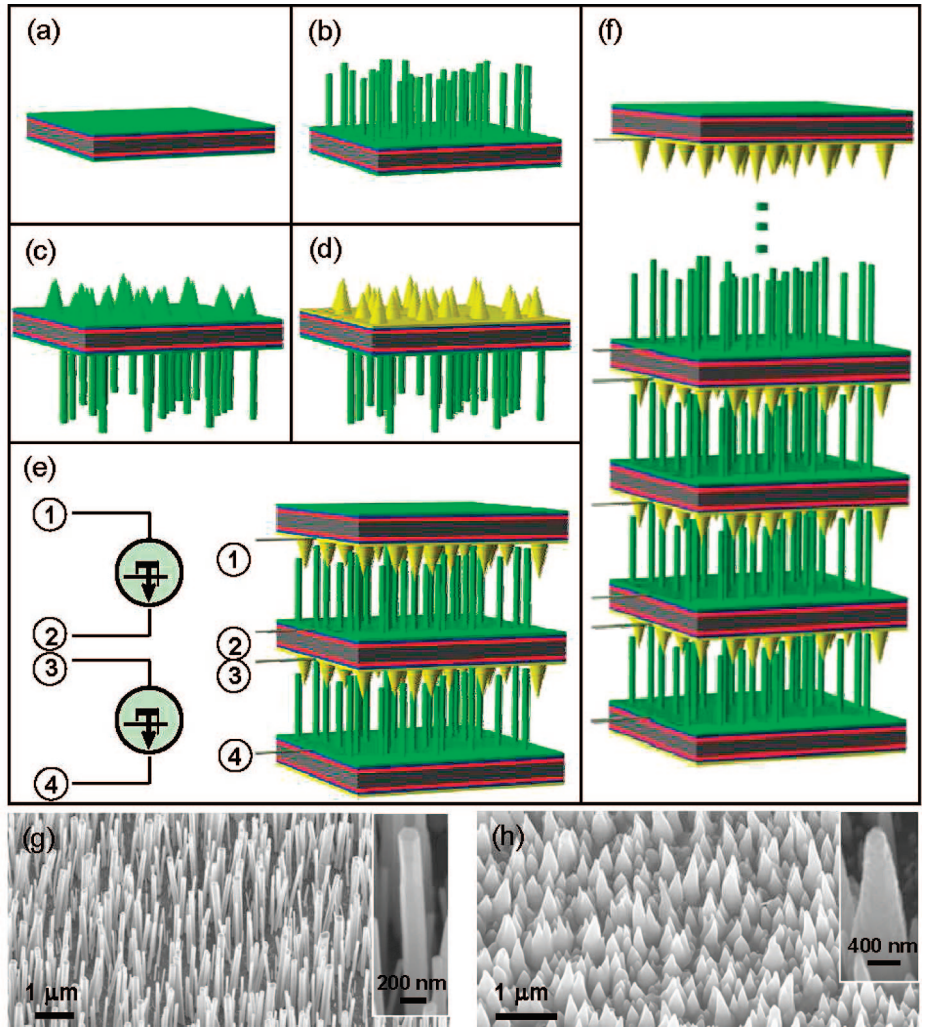

Figure 1. Design and fabrication procedures of the multilayered NGs and rational growth of ZnO NW and NTP arrays. (a) The as-fabricated substrate after coating with the $Zn(CH_3COO)_2$ seed layer. (b) Growth of hexagonal-prism-shaped NW arrays by wet chemical method on one side. (c) Growth of pyramid-shaped NTP arrays on the other side. (d) Coating the NTP arrays with an Au layer by magnetron plasma sputter. (e) Two-layered NG made by stacking three layers of the wafer structures shown in (d), with the Au-coated NTP arrays facing and interpenetrating the bare NW arrays. The right-hand side is the designed symbol for representing the NGs. (f) A multilayered three-dimensional NG integrated by stacking multiple layers of wafer structures. (g) 60° tilt view scanning electron microscopy (SEM) image of the hexagonal-prism-shaped ZnO NW arrays grown by chemical approach. (h) 60° tilted view SEM image of the pyramid-shaped ZnO NTP arrays grown by chemical approach. Inset SEM images are high magnification views of a single NW and NTP.

The aligned ZnO arrays were grown via chemical methods on both sides of the Si wafer with a slight modification to achieve rationally desired morphologies. The wafer was rinsed by 4 °C 0.5 mmol/L $Zn(CH_3COO)_2$ in ethanol solution on both sides[9] and then baked at 350 °C for 15 min to form a layer of (0001) textured ZnO seeds, which leads to the growth of ZnO NWs and NTPs. The density of the ZnO seeds could be varied by using different concentrations of the $Zn(CH_3COO)_2$ ethanol solution. The morphology the ZnO arrays could be manipulated by using different growth temperatures for different lengths of time. Generally speaking, at a low growth temperature and long growth time, NWs were formed (Figure 1b,g), while at a relatively high growth temperature and short growth time, NTPs were grown (Figure 1c,h).[10] The morphology controlled growth of ZnO NW/NTP arrays on different sides of the Si wafer was achieved by floating the substrate on the nutrient solution surface, which is composed of 5 mM 1-to-1 ratio of $Zn(NO_3)_2$ and hexamethylenetetramine, during the growth so that we could apply different growth conditions (the nutrient solution was heated up to 100 °C for 24 h for growing the pyramid-shaped NTPs or 70 °C for 48 h for growing the hexagonal-prism-shaped NWs) independently for either side. Finally, the side with NTPs was coated uniformly with 100 nm thick Au by magnetron plasma sputtering to form a metal tip array.

A NG was made by stacking together two pieces of the grown wafer structures, with the Au-coated NTPs partially interpenetrating into the NWs as illustrated in Figure 1e, and in the same way, a multilayered NG was integrated by stacking multiple layers of such structures layer-by-layer (Figure 1f). The Au-coated NTPs acted like an array of AFM tips, slightly interpenetrating into the spacing between the NWs underneath,[6] just like two face-to-face brushes with a small degree of interdigitative overlap at the ends. Such a design neither has a strict requirement on the height uniformity of the NWs nor needs to maintain a specific gap

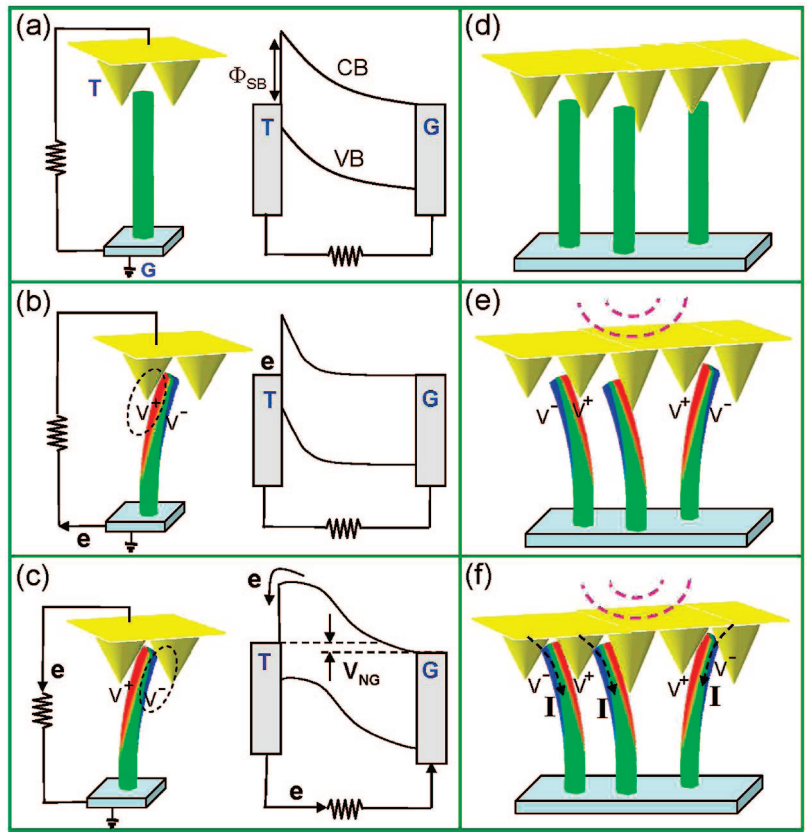

Figure 2. Physical principle of a single-layered NG by considering band diagrams taken from the left/right boundaries of the NW. (a) Schematic diagram of the NG and the corresponding electron energy band diagram, where "T" is the Au−NTP, and "G" is the grounded NW. (b) Under the excitation of ultrasonic wave, there is a relative movement (in both vertical or lateral directions) between the NTP and the NW, and as a result the NW is bent with the contact surface being stretched. The corresponding local piezoelectric potential (positive) creates a reversely biased Schottky barrier. This diagram represents the equilibrium status of the contact between the NTP and NW. (c) When the relative movement of the NTP and NW is strong enough, the NW is bent enough to touch another adjacent NTP with its compressive side. Then, the local piezoelectric potential (negative) sets the Schottky barrier to be forward biased and drives the flow of electrons from the NW into the NTP. If we consider the statistical contribution of thousands of electrons from many NWs, a steady current is formed. This diagram represents the equilibrium status of the energy diagram as many NWs participate in the energy generation. (d) Schematic diagram of multiple NW and NTP contacts with slight variation in heights and lateral distribution. (e) Disregard the NWs being deflected to left-hand or right-hand, the first contacting surfaces with the tips are tensile surfaces with a positive piezoelectric potential. (f) Electric currents created by the driving force of the piezoelectric potential when the compressive surfaces of the NWs contact the surfaces of adjacent tips. The contacts can be simultaneous or with a slight delay, but the created transient currents all flow in the same direction, which is from NTPs to NWs.

distance between the layers, rendering it much easier to control the packaging of the layers.[3] Each layer was insulated from adjacent layers by the Al_2O_3 thin film. After connection to output wires was made, the entire architecture was sealed and packaged by epoxy resin to prevent infiltration of any liquid. The short circuit current was measured by a low-noise current preamplifier (model SR570, Stanford Research Systems). The open circuit voltage was measured by a low-noise preamplifier (model SR560, Stanford Research Systems). In the current generating process, the positive electrode was the side with bare ZnO NW arrays and the negative electrode was the side with Au-coated ZnO NTP arrays.

Several effects could be involved in the energy generation process: triboelectric, pyroelectric, and piezoelectric. The contribution from triboelectric was ruled out by our direct in situ AFM observation of power generation from a single nanowire under optical imaging[11] and our measurements were carried out using nanowires of WO_3, Si, and carbon nanotubes.[3] As for the pyroelectric effect, the temperature in the ultrasonic wave chamber (~1 gallon) was fairly uniform and there was surely no significant temperature gradient across the nanogenerator that had a size of a few millimeters. Furthermore, the response of the nanogenerator to ultrasonic waves was instantaneous when it was turned on and off, as can be seen from the sharp data profile shown in Figure 3. The possible voltage generated by temperature variation across the sample of 6 mm^2 as caused by ultrasonic wave, if any, was extremely small.

The energy conversion process can be understood from the change in local band structure induced by the piezoelectric potential, which is asymmetric across the NW with the stretched side positive and the compressed side negative. Since Au has a work function of 4.8 eV, which is larger than the electron affinity of ZnO (4.5 eV), a Schottky contact (barrier height of Φ_{SB}) at the interface is formed (Figure 2a). The Schottky barrier exists as soon as the NTP is in contact with the NW. When a NTP slowly pushes a NW, a strain field is created across the NW width, with its outer surface

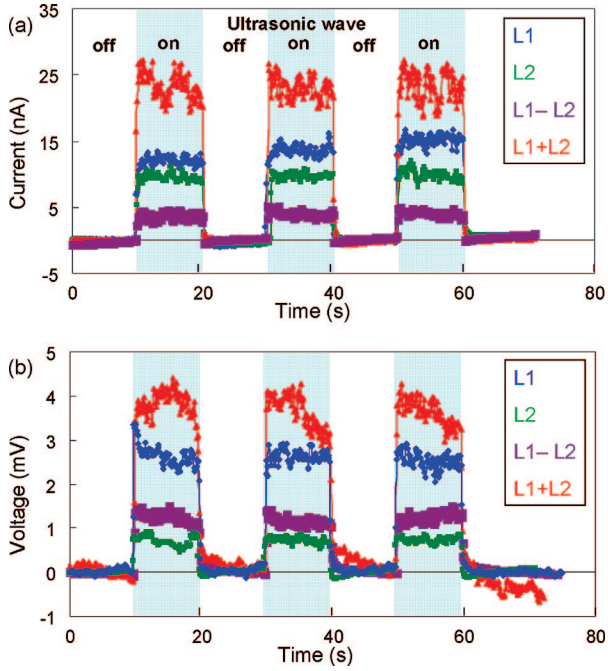

Figure 3. Output current and voltage signals by connecting two single-layered NGs in parallel and antiparallel, and serial and antiserial, illustrating the 3D integration of the NGs for raising output power. (a) Short circuit current output measured from the NGs when connected in parallel and antiparallel. (b) Open circuit voltage output measured from the NGs when connected in serial and antiserial. The regions when the ultrasonic wave was on and off are indicated. The surface area of each NG was 6 mm^2.

in tensile and its inner surface in compressive strain. This asymmetric strain produces an asymmetric piezoelectric potential across its width, with V^- (negative) at the compressive surface and V^+ (positive) at the stretched surface.[3,12] It is important to note that the piezoelectric potential is created by the ions in the crystal when the NW is subject to mechanical deformation, which cannot move freely; they may be partially screened by free carriers in the NW but cannot be completely neutralized or depleted.[13] This means that the piezoelectric potential still preserves even with consideration of the existence of moderate free charge carriers in ZnO NW. When a NTP is in contact with the stretched surface of the NW, which has a higher local potential than the NTP, a reversely biased Schottky barrier (Φ_{SB}) blocks the flow of electrons through the interface (Figure 2b). Because the piezopotential is built up very fast inside the NW[13] as the NTP is pushing the NW, at every moment during the pushing process, the whole system is in an equilibrium state. In other words, if we take a snapshot of every moment of the process, for example Figure 2b, the system is in equilibrium. This is because the flow speed of charges is a lot faster than the scanning speed of the tip. As the degree of NW bending increases, its compressive side may reach the surface of an adjacent NTP; thus, the local piezoelectric potential V^- (negative) in the NW results in a local shape modification of the conduction band of the NW near the NTP (Figure 2c). The piezoelectric potential extends through almost the entire length of the NW according to theoretical calculation,[12] and its most important modification to the band shape is at near the Schottky contact region because of the high-raise of the local band. If the raise in local potential energy is large enough as determined by the degree of NW bending,[12] the accumulated local n-type carriers in the NW can quickly flow through the contact into the NTP, which creates a circular flow of the electrons in the external circuit, e.g., the output current. In terms of a single pair of NTP and NW, this process is transient. But if we focus on the statistical contributions from thousands of NTP/NW pairs, this process is in a steady state, with a stable and continuous current output. The role played by the Schottky barrier is to prevent the flow of electrons from the NTP into the NW, which is a key structure for preserving the piezoelectric potential and releasing the free electrons from the NW into the NTP. A working NG is required to have such a diode effect, and it was first measured for each and every NG to determine its correct polarity (Figures S2 and S3). The role played by the piezoelectric potential is to drive the electrons from the ZnO NW to overcome the threshold energy at the Au−ZnO interface and flow into the Au NTP. The piezoelectric potential does not directly determine the magnitude of the output voltage.

For the ultrasonic wave driven nanogenerator, there were thousands to millions of NWs that contribute to the electric output in a random phase. Although each NW is considered to be in an unequilibrium/trasient state, the statistical average of thousands of them can be considered as in a steady state with a stable and continuous output, which is similar to the process in solar cells, in which a single photon can only crease one or a few electrons that can form an electric pulse, but a continuous current can be formed if thousands of photons strike the cell in random phase. This concept is applied to understanding the output voltage of the NG. As shown in Figure 2c, as more electrons are pumped into the Au NTP, the local Fermi surface is raised by the accumulated electrons with considering the statistical contribution from all of the NWs, as discussed above. Therefore, the theoretical output voltage is dictated by the difference between the Fermi energies of the Au NTP on the top and the ZnO NW at the bottom, as illustrate by V_{NG} in Figure 2c. In practice, one has to consider the contact resistance, system capacitance, and possible current leakage, all of which would lower the voltage output to be measured.[14]

As the NGs were subjected to ultrasonic wave excitation in a water bath, the ultrasonic wave would cause a vertical or lateral vibration of the Si wafers and/or vibration of the ZnO NWs, resulting in a relative bending/deflection of the NWs as enforced by the Au-coated NTPs (Figure 2e). The degree of bending/deflection depends on the intensity of ultrasonic wave. So the variation of ultrasonic wave will cause the change of the output signals, which has been studied by our group and will be published elsewhere. The NTPs were significantly thicker and stiffer than the NWs (Figure 1g,h). Regardless the NWs being deflected to left or right, the currents generated by all of them add up constructively as determined by the Schottky barrier and the uniaxial growth of the NWs (Figures 2e,f),[15,16] although the output voltage is determined by the performance of individual

NWs.[3] A constant and steady direct output current is observed as long as the ultrasonic wave is on.

The layer-by-layer integrated NGs show enhanced output current and voltage. By connection of two individual layers of NG in parallel, e.g., connecting electrodes ① with ③ and electrodes ② with ④ in Figure 1e, the output current was a sum of the two NGs. As shown in Figure 3a, a single layer of NG L1 gave ~13 nA of short circuit output current, and the other layer of NG L2 gave ~10 nA under the same conditions. After the layers were connected in parallel, the output current increased to an average of 22 nA (Figure 3a, red curve). The working principles could be further verified by reversely connecting those two layers of NGs in anti-parallel in reference to the polarities of their Schottky barriers (Figure S2a,b),[17] e.g., connecting electrodes ① with ④ and electrodes ② with ③ in Figure 1e. The total output current was just 3 nA (Figure 3a, purple curve), which was the difference of their individual output currents.[18] As shown in Figure 3a, the output signal for the L1 + L2 case is a lot more "unstable" than that for the L1 − L2 case. This is due to the fact that the L1 + L2 case double amplifies the instability introduced by the intensity and frequency of the ultrasonic wave source, while the L1 − L2 case impairs the instability.

In a similar way, with two layers of NGs connected in serial, e.g., connecting electrodes ② with ③ in Figure 1e, the output voltage was the sum of the output voltages from the two individual layers. As presented in Figure 3b, L1 gave an output voltage of approximate 2.6 mV, while L2 gave about 0.8 mV. When those two layers of NG were connected in serial and tested under the same condition, the output voltage was around 3.5 mV on average (Figure 3b, red curve), which was the sum of their individual outputs. Furthermore, if we put the two layers in antiserial, e.g., connecting electrodes ② with ④ in Figure 1e, the output voltage was just 1.5 mV (Figure 3b, purple curve), which was the difference of their individual output voltages.

Integration of multilayers of NG has great potential for raising the output voltage. Once the output voltage is high enough to operate an electronic device, such as a diode, the outputting electric energy from the NGs can be stored for future use. To demonstrate the technological feasibility of the approach, we have connected several NGs in serial. As shown in Figure 4a, four individual layers of NGs, L3, L4, L5, and L6 with 11, 14, 16, and 20 mV open circuit output voltages, respectively, were connected in serial. The resultant total output voltage was ~62 mV as expected. The corresponding short circuit output current was around 105 nA (Figure 4b). The $I-V$ curves of NGs L3, L4, L5, and L6 are presented in Figure S3. Each of them shows typical Schottky characteristics. It appears that the ultrasonic wave of 41 kHz can penetrate rather deep so that the damping effect is not a major problem. The maximum power output of the four-layer integrated NG is 6.5 nW for a surface area of 6 mm^2. A power density of 0.11 μW/cm^2 was achieved.

The electrical signals measured using the preamplifier system were also examined by an oscilloscope (Tektronix TDS 3014B) to reveal the high-frequency output signal.

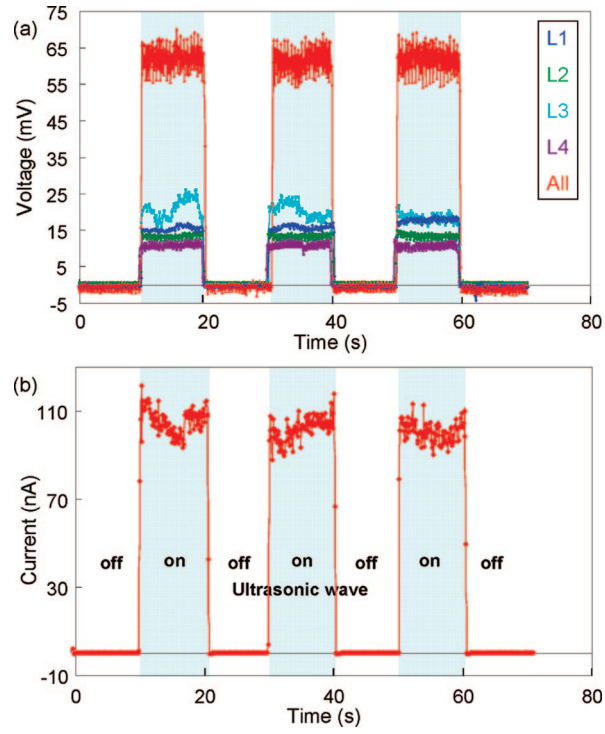

Figure 4. Open circuit voltage and short circuit current output measured from serially connected four-layer integrated NGs. (a) Open circuit voltage output measured from each individual layer and the serially connected four-layer integrated NG. (b) Short circuit current output measured from the serially connected four-layer integrated NG. The regions where the ultrasonic wave was on and off are indicated. The surface area of the NG was 6 mm^2.

Oscilloscope is mainly used to detect periodically oscillating signals. The bandwidth for the oscilloscope in our experiment was 100 MHz. When the ultrasonic wave was turned on, the output signals from our NG as measured by the oscilloscope and the preamplifier system are shown in parts a and b of Figure S4, respectively. The output of the oscilloscope has a steady shift to ~11.5 mV after turning on the ultrasonic wave, although the noise is rather large. This value matches well to the 10.8 mV output measured with the electrical measurement system used in our data acquisition.

In summary, we have demonstrated an innovative approach for fabricating three-dimensionally integrated multilayer NGs for raising the output current, voltage, and power. Aligned ZnO NWs and NTPs were rationally designed to grow on two surfaces of a silicon wafer, respectively. When the surface of NTP arrays was coated with Au, a layer-by-layer stacking of the as-fabricated Si wafers formed an integrated architecture that demonstrated a linear superposition of current and voltage for parallel and serial connection, respectively. This approach has several unique advantages. First, the rational growth of the NWs and NTPs is through wet chemical synthesis at low temperature (<100 °C), which is compatible with other materials and technologies, such as flexible and foldable substrate made of soft materials and silicon-based technologies. Second, the NWs and NTPs do not have to be patterned on substrates in order to raise the output current/voltage, which greatly simplifies the fabrica-

tion process and cost. Third, this design does not demand that all of the NWs and NTPs have a very uniform height and/or shape, greatly reducing the complexity for sample growth. Fourth, the gold coating layer can be replaced by other low-cost metals as long as it can form a Schottky contact with ZnO. The entire fabrication process shows a great potential for scaling up. Fifth, the operation of the NGs relies on mechanical deflection/bending of the NWs, in which resonance of NWs is not required to activate the NG. This largely expands the application of the NGs from low frequency (approximately the hertz range) to a relatively high frequency (approximately the megahertz range) for effectively harvesting mechanical energies in our living environment. Finally, the layer-by-layer assembly provides a feasible technology for building multilayered NGs for applications where force or pressure variation are available, such as a shoe pad, underskin layer for airplanes, and next to a vibration source such as a car engine or tire.

Acknowledgment. Thanks for the support from DARPA (Army/AMCOM/REDSTONE AR, W31P4Q-08-1-0009), BES DOE (DE-FG02-07ER46394), KAUST Global Research Partnership, Emory-Georgia Tech CCNE from NIH, NSF (DMS 0706436, CMMI 0403671). Thanks to Dr. Xudong Wang for many stimulating discussions.

Supporting Information Available: Figure S1 illustrates the fabrication process of the Si wafer before growth of ZnO nanostructures, Figure S2 and Figure S3 show the $I-V$ curves of L1 to L6, and Figure S4 compares the measuring results by oscilloscope and preamplifier. This material is available free of charge via the Internet at http://pubs.acs.org.

References

(1) Tian, B. Z.; Zheng, X. L.; Kempa, T. J.; Fang, Y.; Yu, N. F.; Yu, G. H.; Huang, J. L.; Lieber, C. M. *Nature* **2007**, *449*, 885.
(2) Wang, Z. L. *Sci. Am.* **2008**, *298*, 82.
(3) Wang, X.; Song, J.; Liu, J.; Wang, Z. L. *Science* **2007**, *316*, 102.
(4) Wang, Z. L.; Song, J. H. *Science* **2006**, *312*, 242.
(5) Liu, J.; Fei, P.; Zhou, J.; Tummala, R.; Wang, Z. L. *Appl. Phys. Lett.* **2008**, *92*, 173105.
(6) Qin, Y.; Wang, X. D.; Wang, Z. L. *Nature* **2008**, *451*, 809.
(7) Vayssieres, L. *Adv. Mater.* **2003**, *15*, 464.
(8) Zhang, J.; Sun, L. D.; Yin, J. L.; Su, H. L.; Liao, C. S.; Yan, C. H. *Chem. Mater.* **2002**, *14*, 4172.
(9) Greene, L. E.; Law, M.; Tan, D. H.; Montano, M.; Goldberger, J.; Somorjai, G.; Yang, P. D. *Nano Lett.* **2005**, *5*, 1231.
(10) Xu, S.; Lao, C. S.; Weintraub, B.; Wang, Z. L. *J. Mater. Res.* **2008**, *23*, 6.
(11) Song, J.; Zhou, J.; Wang, Z. L. *Nano Lett.* **2006**, *6*, 1656.
(12) Gao, Y.; Wang, Z. L. *Nano Lett.* **2007**, *7*, 2499.
(13) Gao, Y.; Wang, Z. L. Unpublished results.
(14) Liu, J.; Fei, P.; Zhou, J.; Tummala, R.; Wang, Z. L. *Appl. Phys. Lett.* **2008**, *92*, 173105.
(15) Jasinski, J.; Zhang, D.; Parra, J.; Katkanant, V.; Leppert, V. J. *Appl. Phys. Lett.* **2008**, *92*, 093104.
(16) Lee, S. H.; Minegishi, T.; Park, J. S.; Park, S. H.; Ha, J.; Lee, H.; Lee, H.; Ahn, S.; Kim, J.; Jeon, H.; Yao, T. *Nano Lett.* **2008**, *8*, 2419.
(17) Liu, J.; Fei, P.; Wang, X. D.; Lao, C. S.; Tummala, R.; Wang, Z. L. *Nano Lett.* **2008**, *8*, 328.
(18) Wang, X. D.; Liu, J.; Song, J. H.; Wang, Z. L. *Nano Lett.* **2007**, *7*, 2475.

NL8027813